Nitrite kinetics during anoxia: the role of abiotic reactions versus microbial reduction.

Natalie YN Lim , Åsa Frostegård and Lars R Bakken

Faculty of Chemistry, Biotechnology and Food Science, Norwegian University of Life Sciences, 1432 Ås, Norway

Corresponding author: Lars R Bakken (lars.bakken@nmbu.no)

Keywords

Nitrite kinetics; chemodenitrification; acidic soil; denitrification;

Abstract

Anoxic spells in soil induce denitrification, i.e. the sequential reduction $NO_3^- \rightarrow NO_2^- \rightarrow NO \rightarrow N_2O \rightarrow N_2$, catalysed by the four enzymes NAR, NIR, NOR and NOS, respectively. Transient accumulation of all intermediates is inevitable, but the concentrations depend on the regulation of gene expression and the physical/chemical properties of the soil. Nitrite is chemically unstable at low pH, decomposing via a conglomerate of abiotic reactions with metals and organic compounds which can result in production of NO, N_2O, N_2 and nitrosated organic compounds (R-NO). There is evidence that acidic soils accumulate less nitrite than neutral soils, but it is unclear if this is due to high abiotic decomposition rate (V_{ADEC}) or fast enzymatic reduction of nitrite (V_{NIR}) at low pH. To investigate this, we monitored the kinetics of NO_2^-, NO, N_2O and N_2 during anoxic incubations of three organic soils with pH_{CaCl2} ranging from 3.4 to 7.2, taken from a long-term liming experiment. In parallel, we determined the rate of abiotic nitrite decay (V_{ADEC}) and its product stoichiometry (NO, N_2O and R-NO) in gamma-irradiated soils. V_{ADEC} was clearly first-order with respect to HNO_2 (k_{HNO2} = 1.4 h^{-1}), N-gas production (NO, N_2O and N_2) accounted for only ~50% of V_{ADEC}, the rest was ascribed to nitrosation (R-NO). During denitrification (live soil incubation), the nitrite concentrations reached 2-3 mM in the soils with pH 4.9 and 7.2, while the soil with pH 3.4 kept nitrite concentrations at 20-50 µM , except for a short spike reaching 160 µM. Estimated rates of nitrite scavenging by the two competing sinks (NIR and ADEC) showed that NIR was the strongst nitrite sink in soil with pH 3.4 ($V_{NIR} > V_{ADEC}$), while $V_{NIR} \approx V_{ADEC}$ in the soil with pH 5.9. In the soil with pH 7.2, V_{ADEC} was insignificant. Thus, the regulation of denitrification (high V_{NIR} relative to V_{NAR}) played a crucial role in determining nitrite kinetics, hence the fate of nitrite in acid soils. High nitrite reductase activity effectively minimized abiotic nitrite decomposition and nitrosation of soil organic matter. The results shed light on regulation of denitrification in acid soils, and its implications for the fate of nitrogen during denitrification events.

1. Introduction

Nitrite is a free intermediate in a number of reactions in the nitrogen cycle, including nitrification, denitrification, and dissimilatory nitrate reduction to ammonium [DNRA, also known as respiratory ammonification (Mania et al., 2014; Yoon et al., 2015)]. It is also an important component of the regulatory networks of these metabolic pathways.

While nitrite is relatively stable and only moderately toxic at high pH, its decomposition, reactivity and toxicity escalates with decreasing pH (Bancroft et al., 1979; Van Cleemput and Samater, 1996), reflecting that HNO_2 is more reactive than NO_2^- (pK_a = 3.3 for $NO_2^- + H^+ \leftrightarrow HNO_2$), and that cell membranes are permeable to HNO_2 but not to NO_2^- (Kaiser and Heber, 1983; Samouilov et al., 2007). Metals can catalyse the reduction of nitrite to NO, N_2O and even N_2 (Zhu-Barker et al., 2015). Moreover, HNO_2 can react with various organic compounds (nitrosation and nitrosylation; Spott et al., 2011; Heil et al., 2016). Similar reactions have been proposed for nitrate, but this appear to be due to experimental artefacts (Colman et al., 2007). Finally, nitrite in soils may escape to the atmosphere as gaseous nitrous acid (HONO), and this emission plays an important role in OH formation and tropospheric chemistry (Jacob, 2000; Kulmala and Petäjä, 2011; Su et al., 2011).

Most research on nitrite in soils has focused on the transient accumulation induced by fertilisation with reduced N (urea or ammonium), caused by faster oxidation of ammonia to nitrite than oxidation of nitrite to nitrate. This process is exacerbated by high pH, because nitrite oxidising bacteria are sensitive to NH_3 (Ventera et al., 2015, Breuillin-Sessoms et al., 2017 Shen et al., 2003). However, nitrite has also been observed to accumulate transiently in soil during denitrification (Glass and Silverstein, 1998; Stevens et al., 1998), and peak concentrations appear to increase with soil pH, and the reasons for this are unclear (Shen et al., 2003). It could be due to fast abiotic nitrite decomposition at low pH, but the enzyme kinetics of denitrification could also play a role: early and strong expression of the genes coding for nitrite reductase (*nir*) compared to those coding for NO_3^- reductase (*nar*) in acid soils, would result in marginal accumulation of nitrite. Denitrifying organisms display various regulatory phenotypes regarding the sequence of expression of *nar* contra *nir* (and *nor*, coding for nitric oxide reductase): some organisms reduce all nitrate to nitrite before expressing *nir* and *nor*,

others accumulate some nitrite before reducing it further, and yet others express *nar* and *nir* at the same time and therefore display low nitrite accumulation (Bergaust et al., 2010; Liu et al., 2013; Lycus et al., 2017).

The aim of our investigation was to assess the relative importance of abiotic nitrite decomposition versus the enzymatic nitrite reduction during anoxic spells, as dependent on soil pH. We monitored the kinetics of nitrite and N-gases (NO, N_2O, N_2) during anaerobic incubations of soils of different pH, taken from a long-term field experiment where organic soil had been limed to different pH levels. Soils from this field experiment were used in two previous studies of denitrification product stoichiometry (Liu et al., 2010) and for isolating denitrifying organisms (Lycus et al., 2017). We found the expected pH-dependency of nitrite accumulation: transient nitrite accumulation decreased with pH. To assess the role of abiotic decomposition for the observed nitrite kinetics, we determined the concentration dependent rates of abiotic nitrite decomposition (and the fraction emitted as NO and N_2O) by incubating sterilised soils amended with nitrite. The first order decay kinetics, and the product stoichiometry of this decay was used to assess the abiotic versus enzymatic reduction of N species observed in the live soil. This approach allowed an estimation of the relative strength of the two sinks for nitrite, i.e. abiotic decomposition and enzymatic reduction to NO.

2. Materials & Methods

2.1. Soils

Organic soils were collected from a long-term experimental field site in Fjaler, western Norway (61°17'42"N, 5°03'03"E). The site is divided into 24 plots and limed with shell sand, 0-800 m^3 per hectare (1977) creating a pH range from pH 3.1 to pH 7.8 (Sognnes et al., 2006). The field experiment has been under permanent grassland since established. In this paper, soils from three lime treatments pH were used: soil **L** (un-limed soil, pH 3.16-3.80), soil **M** (medium lime; 200 m^3 shell sand per hectare, pH 5.79-5.89), and soil **H** (high lime; 800 m^3 shell sand per hectare, pH 6.77-6.80). Soils from this field experiment were used previously to determine the effect of soil pH on the denitrification product stoichiometry (Liu et al., 2010), and for isolating representative culturable denitrifying organisms (plot L and H; Lycus et al., 2017).

Two replicate plots were sampled from treatments L and H; and one plot from treatment M. The soil from each plot was analysed separately. Only one plot was sampled from M because shell sand was unevenly distributed in the replicate plot, resulting in a pH that was too close to soil L for our purposes (the pH at the time of sampling was 4.34). All pH values were measured in 0.01 M $CaCl_2$ [1:5 w/w, soil fresh weight (fw) to 0.01 M $CaCl_2$] prior to using the soil. The soil organic C contents were 49, 45 and 40 % of dry weight (dw) in soil L, M and H, respectively. The declining C content with increasing pH was primarily due to the increasing amounts of shell sand added in 1977.

The soils were nearly water saturated when sampled (taken during the rainy season), and were immediately dried to reach a moisture level that allowed sieving (8 mm, followed by 4 mm). Large roots and plant residues were removed during the drying process, and the soils were frequently mixed by hand to avoid edge effects. The sieved soils were stored moist [61, 59 and 46 % moisture (w/w) in soil L, M and H, respectively] at 4 °C until use. The water holding capacity (WHC) of each soil was determined by flooding and free drainage in filter funnels; WHC was 82, 78 and 68 % moisture (% of fw) for soil L, M and H, respectively.

2.2. Soil sterilisation

Soil samples were sterilised by gamma-irradiation, to determine the abiotic kinetics of NO_2^- decay and the product stoichiometry of this process. The choice of gamma sterilisation, rather than autoclaving was based on a comparison of gamma sterilisation, chloroform fumigation and autoclaving as to their elimination of biological activity and effects on abiotic NO_2^- decay to NO (described in: Supplementary material S1: Comparison of sterilisation methods).

The soils were given a dose of 27.8 kGy (^{60}Co) (at the Institute of Energy Technology, Kjeller, Norway). The gamma-irradiated soil was stored for 3 months at 4 °C before use, to deplete free radicals generated by radiolysis.

2.3. Nitrite measurements

To monitor the fast degradation of nitrite in the acidic soils, a quick method for measuring nitrate and nitrite was developed. Briefly, 0.2-0.5 g of soil (fw) was transferred to pre-weighed microcentrifuge tubes for nitrite measurement, and sterile MilliQ water (1:2 w/w, soil fw to water) was added to extract the nitrite from the soil matrix. The soil slurry was agitated with a

vortex mixer for 5-10 s, then the soil solids were pelleted by centrifugation (17 600 x *g* for 2 min). Then 10 µL of the supernatant was immediately injected into a purging device where nitrite or nitrate+nitrite (depending on reducing agent and temperature) was instantaneously reduced to NO which was transported (by a stream of N_2) through a Sievers Nitric Oxide Analyzer 280i system (NOA, GE Analytical Instruments). The integrated NO peaks were used to estimate nitrite and nitrite+nitrate in the injected sample (calibrated by injecting standards). The reducing agents and temperatures were 1 M HCl with ≈50 mM VCl_3 (95 ^oC) to reduce nitrite+nitrate, and 1 % w/v NaI in 50 % acetic acid (room temperature) to reduce only nitrite. This chemiluminescence nitrate and nitrite measurement is capable of detecting picomole quantities in the injected liquid (Braman and Hendrix, 1989; Cox, 1980).

We suspected that the fast extraction with water could be affected by anion exchange, and tested this by comparing our water extraction procedure with the standard extraction in 2 mM KCl. This comparison was done for nitrate, rather than nitrite, since KCl is suspected to cause degradation of nitrite under acidic and neutral pH conditions (Homyak et al., 2015). The amount of nitrate extracted in water was 50-60 % of that extracted by 2 mM KCl (Supplementary Table S1), thus confirming a significant anion exchange capacity of the soils, leading to the recovery of only 50-60 % of the nitrate when using our rapid water extraction procedure.

To determine the kinetics of anion exchange, we measured the recovery of nitrite added to gamma-irradiated soils in short-term experiments. Microcentrifuge tubes containing 0.2 g soil fw (≈30 % dw) were given a dose of 100 nmol NO_2^- (10 µL of 10 mM KNO_2), and extracted with water at different time points during the first 10 min. The measured concentrations showed a rapid decline during the first 5 min in all soils, approaching apparent equilibrium levels (50-60 % recovered) after 8-10 min (Supplementary material, Fig. S2). The concentration dependency of this anion partitioning (sorbed/free anions) was tested by adding a range of nitrite concentrations (50-1000 nmol per vial containing 0.2 g soil fw) which was extracted after 10 min. The fraction of nitrite recovered in the water extract (*F*) was practically constant over the entire concentration range for the two soils tested, *F*=0.49 and 0.65 for L and H, respectively (Supplementary material Fig. S3). These values were used for correcting the nitrite concentrations as measured in subsequent experiments (assuming an intermediate *F* value of 0.57 for soil M).

2.4. Kinetics of nitrite decomposition and gas production in gamma-irradiated soils

Gamma-irradiated soils were used to determine the kinetics of abiotic nitrite decay and the gas products. A first approach to determine nitrite decay under aerobic conditions was a 5 h experiment in microcentrifuge tubes. Nitrite was added (10 µL of 10 mM NO_2^- = 100 nmol NO_2^- $vial^{-1}$) to a series of microcentrifuge tubes containing 0.2 g fw soil (≈0.1 g dw), and residual nitrite was measured at intervals using the rapid water extraction procedure described above. The length of the experiment proved too short to determine the decay rate in soil M and H, hence a longer-term experiment was conducted in which gamma-irradiated soils supplemented with nitrite under oxic and anoxic conditions in serum vials at 15°C. Anoxic conditions were secured by repeated evacuation and He-filling. Oxic vials received an injection of O_2 to reach 21%. Each vial, containing 2 g soil, was amended with nitrite by spreading 0.1 mL of 10 mM KNO_2 onto the soil surface by a syringe. For each of five soils (2 replicates of L and H, a single for M), we prepared six 120 mL vials (3 oxic, 3 anoxic) which were monitored for gas production (NO, N_2O and N_2), and 22 small (12 mL) replicate vials (11 oxic and 11 anoxic) which were sacrificed consecutively (every 5 h) to determine the concentration of nitrite. The 120 mL vials were placed in the incubation robot, which monitored the N_2, N_2O and NO concentrations in the headspace by gas chromatography (N_2 and N_2O) and chemiluminescence (NO), described in detail by Molstad et al. (2007). The nitrite addition to the 120 mL vials was done to each individual vial <1 min before the first gas sampling of the same vial. The 22 small vials were prepared and treated the same way as the larger vials. Nitrite concentrations were determined by rapid water extraction of all the soil within the vial (adding 5 mL distilled water), corrected for the partitioning due to ion exchange (F = 0.49, 0.57 and 0.64 for soil L, M and H, respectively).

2.5. Kinetics of denitrification in live soils

Prior to the determination of denitrification kinetics in unsterilised soils, they were revitalised from cold storage as described by Liu et al. (2014). The soils were amended with 5 mg dried, powdered clover g^{-1} soil fw and incubated at 15 °C for 72 h. They were then transferred to 120 mL serum vials. The amount of soil was adjusted to have 1.5 g soil organic C per vial (fw equivalent to 3.06, 3.33 and 3.75 g soil dw $vial^{-1}$ for L, M and H, respectively). After sealing the vials with butyl-rubber septa and aluminium crimps, nitrate solutions were added by syringe

onto the soil surface. The vials were then gently agitated to assist in mixing the soil (so not all the nitrate would be on the surface). The volumes and nitrate concentrations were adjusted for each soil to achieve a final water content of 80 % of the WHC (i.e. 66, 63 and 54 % moisture (w/w), soil L, M and H respectively) and 5 mM nitrate in soil moisture. This planning was based on nitrate concentration measured prior to revitalisation, which turned out to be lower than that at the onset of incubation (determined by subsamples that were analysed at the onset of incubation). The reason is most probably nitrification during the revitalisation period. Thus, at the onset of the incubation, the nitrate concentrations in the soil moisture was 6.2, 7.7, and 7.1 mM in soil L, M, and H, respectively, and the total amount of nitrate per vial was 37, 40 and 26 μmol nitrate (L, M and H respectively).

The vials were made anoxic by 6 cycles of gas evacuation and helium filling (Liu et al., 2010), and incubated at 15 °C. Gases (CO_2, O_2, NO, N_2O and N_2) in the headspace were measured every three hours using the incubation robot mentioned earlier (Molstad et al., 2007). At each gas sampling time point, one replicate vial of each soil type was opened and soil nitrite was measured.

2.6. Gas measurements and kinetics

Gas concentrations and the kinetics of gas turnover was measured by the robotized incubation system described in detail by Molstad et al. (2007). In short, the system consists of a thermostated water bath with racks for holding 120 mL serum vials with crimp-sealed butyl rubber septa (the original system hosts 21 vials, while the improved version (Molstad et al., 2016) hosts 46 vials). The headspace of the vials is sampled repeatedly throughout by piercing the septa with a thin needle coupled to a peristaltic pump transporting the sample to the sampling loops of the analytic system, and pumping back an equal volume of He to secure ~ 1 atm pressure in the vials. The analytic system consists of a gas chromatograph (analysing O_2, N_2, N_2O) and a chemiluminescence NO detector. The system allows determination of the rate of gas production/consumption for each time interval between two samplings, taking the dilution by sampling and the inevitable but miniscule leakage of N_2 and O_2 into account. The leakage is primarily through the injection system (peristaltic pump), and amounts to 50 nmol N_2 for each sampling. The leakage varies somewhat between experiments, dependent on wear and tear of the peristaltic tubing, but is measured in each experiment by including empty vials (with He only) in each experiment. Leakage through the septa is negligible even after many samplings because the needle never pierces the septum in the same place twice. Gas

concentrations in 12 mL vials prior to destructive sampling were measured with the same systems.

3. Results

3.1. Nitrite decay and N gas kinetics in gamma-irradiated soils

The measured kinetics of nitrite anion exchange with the soils demonstrated that it took less than 10 min to reach equilibrium between free and adsorbed nitrite (Supplementary Fig. S2). In principle, the kinetic constants for ion exchange and nitrite decay could be determined by fitting a model that includes both phenomena, as demonstrated in Supplementary Fig. S4. This exercise established, however, that the necessity of taking the kinetics of ion exchange into account is limited to the first 10 min after addition of nitrite. Hence, the measured nitrite >10 min after nitrite addition could be corrected for the soil specific partitioning at equilibrium. Table 1 summarises the partitioning and the estimated first order decay rates of nitrite in the gamma-irradiated soils (graphical presentation in Supplementary Fig. S5). For soil H, the estimated first order decay rate was extremely low (large standard error; Fig. S5, Table 1). The decay during oxic incubation appeared to be somewhat faster than for anoxic incubation (Fig. S6).

Plotting the first order decay rates against the fraction of un-dissociated HNO_2 (given pK_a = 3.398) revealed a linear relationship (r^2 =0.999, Supplementary Fig. S7), suggesting that the decay of nitrite in all soils can be described by a first order decay of un-dissociated HNO_2 with the decay rate constant k_{dHNO2}=1.43 h^{-1}. Thus the decay rate of total nitrite (TONI = NO_2^- + HNO_2) in a soil is given by equation (1)

$$\frac{d[TONI]}{dt} = 1.43 * [HNO_2] = 1.43 * [TONI] * (\frac{[HNO_2]}{[HNO_2]+[NO_2^-]}) \qquad (1)$$

where [X] is the concentration if component X, and the concentration of HNO_2 is a function of pH ($[HNO_2]/([HNO_2]+[NO_2^-]=1/(1+10^{pH-pKa})$, where p$K_a$= 3.398).

Table 1
Decay rate of NO_2^- in gamma-irradiated soils under anoxic conditions. The table shows soil pH, the partitioning of nitrite ions during water extraction, R = estimated ratio between NO_2^- in the distilled water and NO_2^- adsorbed to soil particles after extraction with distilled water, WF = fraction of NO_2^- in the water ($=R/(R+1)$), and k_d = the estimated first order decay rate constant (h^{-1}) under anoxic conditions (standard error in parenthesis).

Lime treatment	pH	R	WF	k_d (h^{-1})
L	3.44	0.77	0.44	0.73 (0.065)
M	4.90	0.74	0.43	0.057 (0.007)
H	7.24	1.37	0.58	0.00055 (0.002)[a]

[a] The decay rate for soil H is not significantly different from zero.

Gamma-irradiated samples of soil L, M and H, with and without nitrite, were incubated in a He (O_2-free) atmosphere and monitored for NO, N_2O and N_2 emissions by sampling every 5 h for 135 h. The N_2 production was below detection limit for all soils (Supplementary Table S2). In contrast, nitrite clearly enhanced the emission of NO and N_2O from the gamma-irradiated soil, as shown in Fig. 1, where cumulative production of the two gases is plotted against time, together with the cumulative nitrite decomposition as predicted by the first order decay rates (Table 1). The nitrite-induced NO production clearly coincided with the decay of nitrite, while the nitrite-induced N_2O production continued beyond the depletion of nitrite (soil L and M). The fraction of decomposed (lost) nitrite recovered as NO during the first 10 h of incubation was 0.53, 0.52 and 0.20, for soil L, M and H, respectively. The fraction remained stable for soil L, declined slightly towards the end of the 135 h incubation for soil M (Supplementary Fig. S8), and for soil H there was an increasing trend. The fraction of decomposed (lost) nitrite recovered as N_2O during the first 10 h was 0.02, 0.078 and 0.17 for soil L, M and H, respectively. This fraction increased gradually with time for all soils.

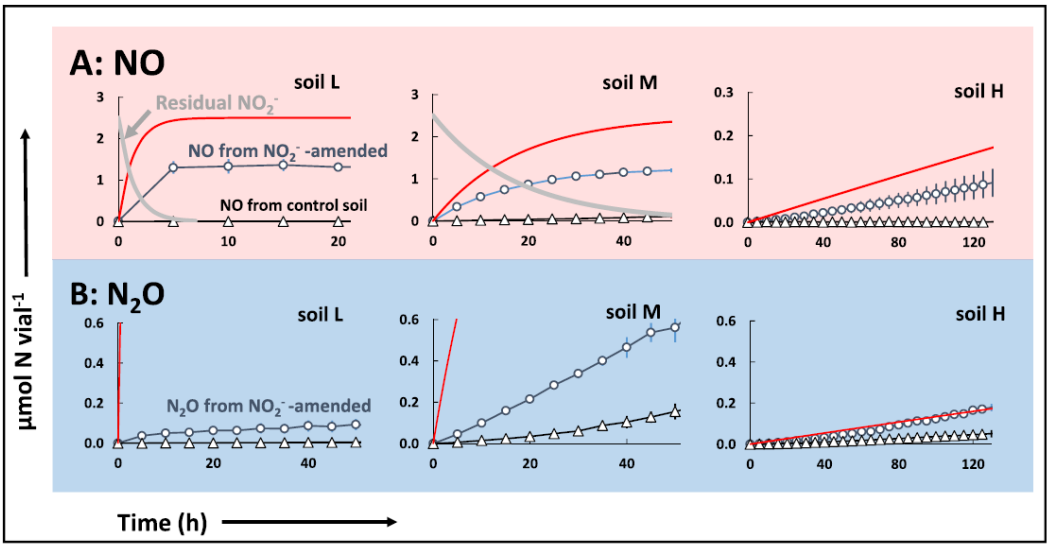

Fig. 1. Nitrite (NO_2^-) decay, NO and N_2O production in gamma-irradiated soil L (pH 3.4), M (pH 4.9) and H (pH 7.1). The panels show cumulative production of NO (A) and N_2O (B) in nitrite amended soil (2.5 µmol NO_2 to 10 g soil fw in each vial). The residual nitrite, as predicted by the first order decay is shown as grey curves, and the red curves show the cumulative nitrite decay. Residual nitrite in soil H remained high throughout (Fig. S5), and is not visible due to scaling. For comparison, the NO- and N_2O-production in control soils (no nitrite added) are shown as triangles (◊) Note that the scales are different and only the first part is reported for soil M and L to enhance visibility. Results for the entire incubation for all soils is found in Supplementary Fig. S8.

.

In order to use the abiotic nitrite decay kinetics (and the N gas production) when analysing the result of the nitrite kinetics in live soil (see below), we had to assume a constant product stoichiometry, and decided to use the fractions recovered as NO and N_2O and R-NO (f_{NO}, f_{N2O} and 1-f_{NO}-f_{N2O}, respectively, see Fig. 2) at the time when ~ 50% of the nitrite had disappeared for soil L and M, and after 10 h incubation for soil H. By R-NO we mean nitrosated nitrite-N as inferred by the N mass balance.

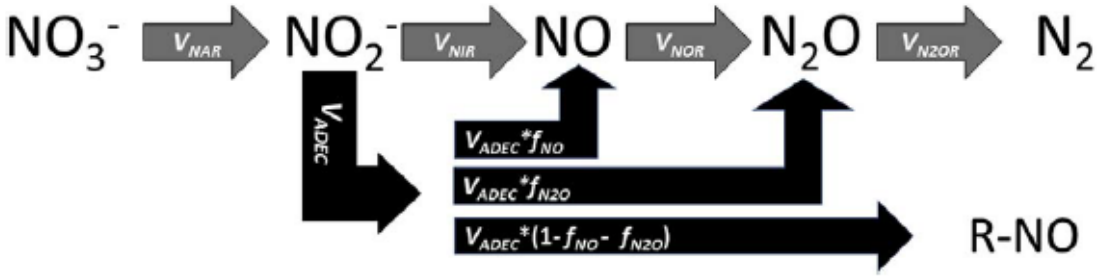

Fig. 2. Calculations of enzymatic and abiotic transformations. Enzymatic transformations are denoted by grey arrows. Abiotic transformations (black arrows) were estimated based on measured concentrations of nitrite, the first order decay, and partitioning, as observed in gamma-irradiated soils. This allowed the estimation of enzymatic reduction rates based on the measured rates of change in NO_2^-, NO, N_2O and N_2 (equations (2)–(7)). V_{NAR}, V_{NIR}, V_{NOR}, and V_{N2OR} are the rates of enzyme-mediated reactions. V_{ADEC} is the predicted rate of abiotic nitrite decomposition. R-NO is the nitrosated/nitrosylated organic compounds.

3.2. Kinetics of denitrification in unsterilised soils, enzymatic reduction of nitrate versus abiotic decomposition.

Samples of unsterilised soil L, M and H were incubated under anoxic conditions with nitrate, and monitored for N-gas production. Parallel soil samples were treated identically in a series of vials which were analysed for nitrite (destructive sampling) at regular intervals.

The kinetics of NO_2^-, NO, N_2O and N_2 for the three soils are shown in the top panels in Fig. 3. The cumulative N_2 reached plateaus at 24.5, 32 and 25 μmol N_2-N $vial^{-1}$ for soil L, M and H, respectively. In comparison, the initial amounts of nitrate was 37, 40 and 26 μmol $vial^{-1}$. Thus, the percentage of initial nitrate-N accounted for as N_2 was only 66, 80 and 96 % for soil L, M and H, respectively. The cumulative N_2-N as calculated is corrected for the N_2 lost by sampling, but not for the sampling loss of NO and N_2O. Taking these losses into account, the estimated total N recovery as N-gas production increased to 28.6, 34 and 26.1 μmol N $vial^{-1}$ for the tree soils (Table 2), which accounts for 77, 80 and 100% of the initial amounts of nitrate.N in soil L, M and H, respectively.

The measured rate of change in NO_2^-, NO, N_2O and N_2 were assumed to be the net result of abiotic nitrite decomposition and enzymatic reductions, as illustrated in Fig. 2. We assumed abiotic nitrite decomposition to follow the first order decay and its partitioning (to NO, N_2O and R-NO) as in gamma-irradiated soil, which was thus predicted by the measured concentration of nitrite and the decay rate constants (Table 1). Thus, the measured rates of change for each N species (dNX/d*t*) and the concentration of nitrite could be used to estimate

the rates of enzymatic reductions (V_{NAR}, V_{NIR}, V_{NOR} and V_{N2OR}, denoting the rates of enzymatic reduction of NO_3^-, NO_2^-, NO, and N_2O, respectively) for each time increment. This was done consecutively through equations 2-5:

$$dN_2/dt = V_{N2OR} \quad (2)$$

$$dN_2O/dt = V_{NOR} + V_{AN2O} - V_{N2OR} \quad (3)$$

$$dNO/dt = V_{NIR} + V_{ANO} - V_{NOR} \quad (4)$$

$$dNO_2^-/dt = V_{NAR} - V_{NIR} - V_{ADEC} \quad (5)$$

where V_{NAR}, V_{NIR}, V_{NOR} and V_{N2OR} are the unknowns, dNX/dt is the measured rate of change of compound N_X, V_{ADEC} is the rate of abiotic nitrite decomposition as predicted by the measured nitrite concentrations, and the first order decay rates ($[NO_2^-]*k$, V_{ANO} and V_{AN2O} are the rates of NO and N_2O production by abiotic nitrite decomposition and the fractions emitted as NO (f_{NO}) and N_2O (f_{N2O}), equations 6-7:

$$V_{ANO} = V_{ADEC}*f_{NO} \quad (6)$$

$$V_{AN2O} = V_{ADEC}*f_{N2O} \quad (7)$$

where f_{NO} = 0.53, 0.52 and 0.2 for soil L, M and H, respectively, and f_{N2O} = 0.02, 0.078 and 0.17 for soil L, M and H, respectively.

The resulting V_{ADEC} and V_{NIR} are shown in the lower panels of Fig. 3. For soil L, abiotic decomposition accounted for only 20-30 % of the total nitrite scavenging during the first 30 h, but as V_{NIR} declined (coinciding with the onset of N_2O reduction), abiotic decomposition became the dominant sink for nitrite. In soil M, we see a similar pattern, but here the abiotic decomposition gained momentum earlier, and essentially equalled V_{NIR} until depletion of nitrite. In contrast to these two soils, abiotic decomposition of nitrite in soil H was insignificant throughout.

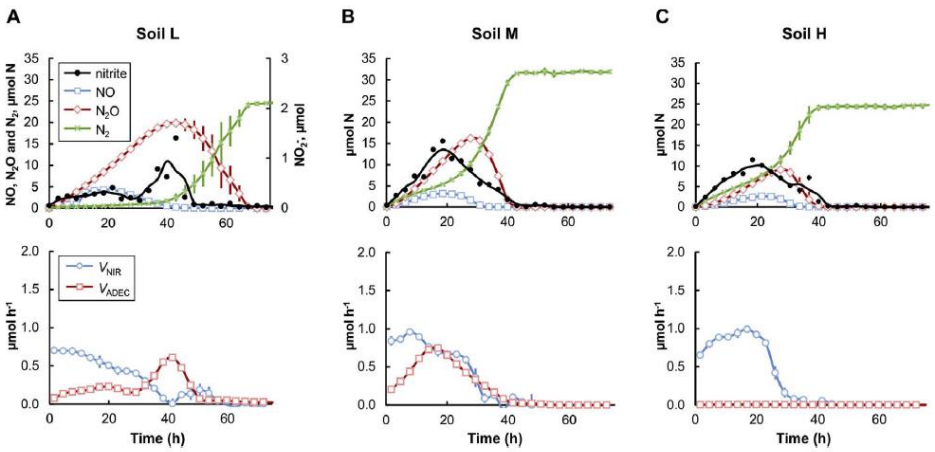

Fig. 3. Kinetics of denitrification and evaluation of abiotic NO_2^- decomposition versus enzymatic reduction of NO_2^-. Top panels show the measured NO_2^- (single measurements and floating average as black circles and lines, respectively), together with measured NO and N_2O and cumulative N_2 production (i.e. corrected for dilution by sampling), and are averages of three replicate vials (standard deviation as vertical lines). The lower panels show the estimated rates of enzymatic nitrite reduction (V_{NIR}) and the rate of abiotic nitrite decomposition (V_{ADEC}); see text for explanation.

To inspect if abiotic nitrite decomposition in soil L and M could explain why less than 100 % of the nitrate-N was recovered as N-gas in these soils (see above), we calculated the nitrate-N balance for each soil, including the abiotic formation of nitrosated/nitrosylated organic compounds, R-NO (Fig. 2, Table 2). The latter was estimated as the integral of V_{ADEC} multiplied by the fraction which was not recovered as N gas ($= \int V_{ADEC} dt^* (1 - f_{NO} - f_{N2O})$; $\int V_{ADEC}$ = 14 and 17.1 µmol N, and $f_{NO} + f_{N2O}$ = 0.55 and 0.6 µmol N for soil L and M respectively). Based on our calculations, we were able to account for all nitrate-N in soil M and H, and 94 % of nitrate-N in soil L (Table 2).

Table 2
Nitrate N mass balance. The table shows the recovery of NO_3^--N as N gases (NO, N_2O and N_2) and as R-NO (abiotic reactions with soil organic matter, Fig. 2). The bottom row shows the total recovery (% of NO_3^--N in parenthesis).

	Soil L	Soil M	Soil H
Initial NO_3	37.0	40.0	26.0
N_2	24.5	32.0	25.0
Sampling loss[a]	4.1	2.0	1.1
N-gas, total (N_2 + sampling loss)	**28.6**	**4.0**	**26.1**
R-NO[b]	14*0.45 = 6.3	17*0.4 = 6.8	0.14*0.4 = 0.06
N accounted for	**34.9**	**40.8**	**26.2**
%	**94%**	**102%**	**101%**

[a] The cumulative N_2 as estimated (Fig. 3) includes the sampling loss of N_2, but not the loss of NO and N_2O. To estimate the total amount of N-gas, the cumulative sampling loss of N_2O and NO were added.

[b] The amount of nitrosated soil organic matter (R-NO) produced, estimated as the product of the cumulative abiotic nitrite reaction (V_{ADEC}) and the R-NO-fraction ($=1-f_{NO}-f_{N2O}$) observed in gamma-sterilized soil (see text for further details).

To inspect the kinetics of the various reductase reactions and the total respiratory electron flow, equations 1-4 were used to calculate the rates of the individual reductases and the total electron flow to denitrification throughout the entire incubation (Fig. 4). A conspicuous phenomenon revealed by these graphs is that in soil L and M, V_{NIR} declined substantially at the time when N_2O-reduction gained momentum. This decline in V_{NIR} was clearly not a result of nitrite depletion (see Fig. 3).

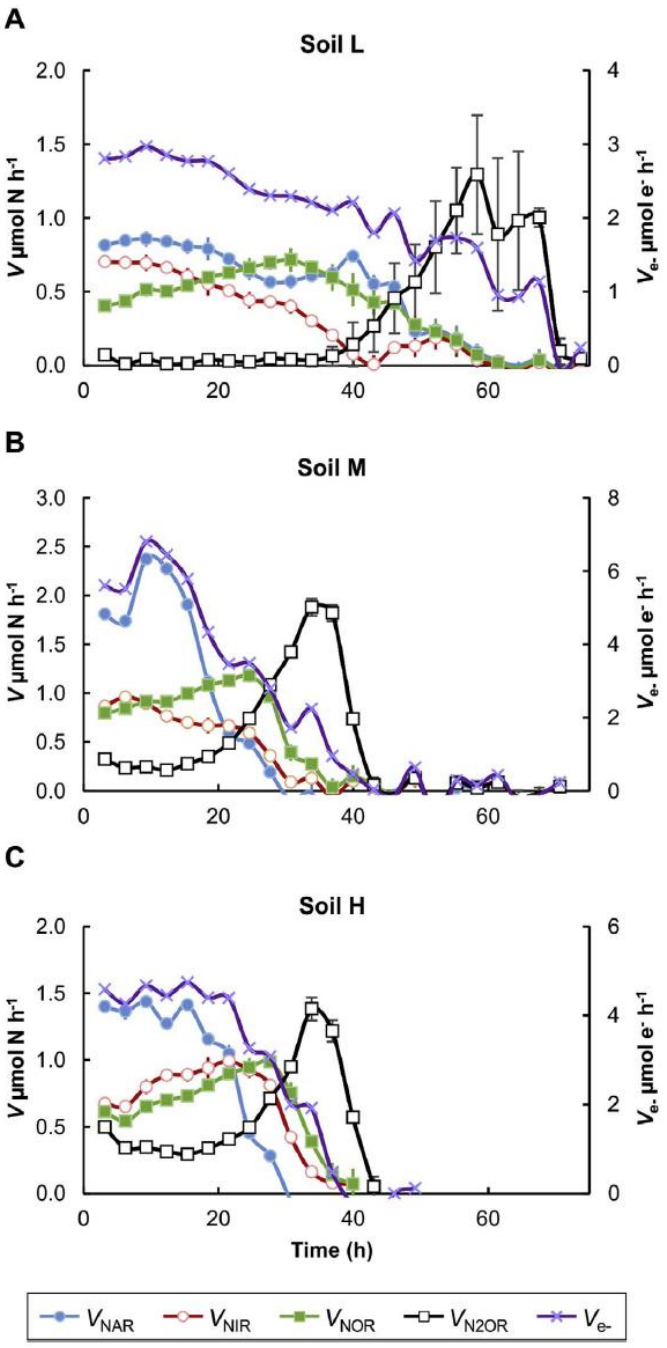

Fig. 4. Rates of individual reduction steps in denitrification. The panels show the rates of nitrate reduction (V_{NAR}), nitrite reduction (V_{NIR}), NO reduction (V_{NOR}) and N_2O reduction (V_{N2OR}), all as µmol N $vial^{-1}$ h^{-1}. In addition, the total electron flow to denitrification is shown (V_{e-}, right axis), as µmol electrons $vial^{-1}$ h^{-1}. The rates were based on measured net rates of production/consumption for each gas, and the rates of abiotic nitrite decay, solved for individual enzyme reactions through equations (2)–(7).

4. Discussion

As underscored by Ventera and Rolston (2000a), the abiotic nitrite transformations must be taken into account in order to determine/understand the kinetics of biological nitrite transformations in soils. The significance of the abiotic nitrite reactions was convincingly demonstrated in several investigations of the transient nitrite accumulations in aerobic soils, as induced by fertilization (Ventera and Roston, 2000b, Ventera et al., 2005 & 2015). Our investigation is analogous to these investigations, focusing on the transient nitrite accumulation induced by anoxic spells, attempting to discriminate between the abiotic and biotic nitrite transformations as illustrated in Fig 2. The kinetics of nitrite decomposition in these soils, as determined in gamma-irradiated soils, was convincingly first order, with decay rate constants that correlated strongly with the fraction of un-dissociated HNO_2. Thus, we have confirmed that soil pH is a good predictor of the abiotic nitrite decomposition rate in soil, given by Equation 1 and the pH dependent equilibrium $NO_2^- + H^+ \leftrightarrow HNO_2$. Similarly, Ventera and Rolston (2000) determined the first order kinetics of abiotic transformation of HNO_2 to NO under oxic conditions, and obtained rate constants ranging from 1-1.4 µg NO-N $µg^{-1}$ HNO_2-N

h^{-1}. These rate constants are indeed very close to what we have estimated for the abiotic HNO_2 reactions under anoxic conditions: Our first order decay rate constant for HNO_2 (1.4 h^{-1}), and the product stoichiometry (~50% NO) implies a first order abiotic NO-production rate of 0.7 µg NO-N $µg^{-1}$ HNO_2-N h^{-1}, which is comparable (albeit somewhat lower) than the rate constants determined by Ventera and Rolston (2000).

The immediate gaseous products of HNO_2-decay was ≈50 % NO and a lower percentage of N_2O (that increased with soil pH), while N_2 production was marginal (not detectable). Hence, the formation of nitrosated soil organic N (R-ON) accounted for a significant fraction of the HNO_2-decay observed. Subsequent decay of R-ON could potentially account for the observed nitrite-induced N_2O emissions beyond the depletion of nitrite in soil L and M (Fig. 1 and Supplementary Fig. S8). This process has previously been defined as co-denitrification, and the N_2O (and N_2) produced is called hybrid N_2O (N_2) because only one of the N atoms stem from nitrate/nitrite (labelling experiments). Since N_2O was the only hybrid product in our experiment (no N_2 was produced), this process is probably dominated by the nitrosation of amines, which are thought to decay to N_2O (Spott et al., 2011).

Using these abiotic nitrite decay rates and the product stoichiometry, the biological enzymatic rates (V_{NIR}) and the abiotic nitrite decomposition rates (V_{ADEC}) during anoxic incubation of live soils were determined (Fig. 3). These estimated rates of enzymatic versus abiotic nitrite decay demonstrated that abiotic nitrite decay could not account for the very low nitrite accumulation in the unsterilised acid soil L. In this soil, the microorganisms clearly kept nitrite concentrations low by high NIR activity compared to that of nitrate reductase (NAR), except for the brief period after 30 h. Interestingly, this coincided with increasing N_2O reduction (N2OR), suggesting that N2OR was able to compete with NIR for available electrons (since the total electron flow V_{e^-} remained essentially unchanged, Fig. 4). In soils M and H, NAR activity greatly exceeded that of NIR initially, resulting in the high transient nitrite accumulation observed (Fig. 3). As nitrite accumulated in soil M, the rates of abiotic nitrite decomposition increased to practically the same level as the enzymatic nitrite reduction. In soil H, however, the abiotic decomposition of nitrite played no role.

Thus, in soils M and H, there was a preferential initial reduction of nitrate over nitrite; while in the very acidic soil L, nitrite reductase was more active from the very early phase of the anoxic

incubation. In theory, this could reflect that the soils harbour different denitrifying communities, i.e. that nitrite accumulates in soil L and M because organisms with the genes for nitrate reductase (nar) are more numerous than those with genes for nitrite reductase (nir), while less nitrite accumulates if soil L due to a high frequency of cells with *nir*. Interestingly, the attempts to isolate representative culturable denitrifying organisms from the same soils (Lycus et al., 2017) show exactly this pattern: the fraction of isolates with *nar* (with or without the other denitrification genes) were 0.9 and 0.6 for soil H and L, respectively, while the fraction of isolates with *nir* (with or without the other denitrification genes) were 0.42 and 0.55 (H and L, respectively). This may be coincidental, however, because full-fledged denitrifying organisms display a wide variety of regulatory phenotypes with respect to nitrite accumulation, even among closely related strains (Liu et al., 2013). Thus, regulatory biology is possibly overruling gene abundance in determining the kinetics of nitrite. The regulatory network controlling denitrification gene expression in most organisms include substrate induced transcription of *nir* (van Spanning et al, 2007), and it appears likely that this induction is strengthened by low pH since the cell membrane is permeable to HNO_2, but not to NO_2^-. This is all very speculative, but warrants a closer inspection of how pH controls the regulation of denitrification in individual organisms.

Needless to say, the calculated nitrogen flows via denitrification and abiotic decomposition of nitrite is based on the assumption that the nitrite decomposition kinetics (and its product stoichiometry) observed in the gamma-irradiated soil is representative for the abiotic processes in the non-sterilised soil. We have no proof for this assumption, but find it rather plausible based on the nitrate N mass balance calculations: around 20 % of the nitrite N was not recovered as N-gas in soil L and M, but the inclusion of the estimated formation of nitrosated soil organic N could effectively account for this missing nitrate-N. In soil H, the estimated nitrite decomposition was insignificant, and as expected, 100 % of the nitrite N was successfully recovered as N-gas. In theory, dissimilatory reduction of nitrite to ammonium (DNRA) could have accounted for some of the missing nitrate-N in the soil L and M. However, DNRA has been found to be negligible in acidic soils compared to that in neutral and alkaline soils (Zhang et al., 2015). In our experiments, DNRA appears to be an insignificant sink, even in soil H (pH 7.24), considering the 100 % recovery of nitrate-N as N-gas. A reasonable conclusion is therefore that DNRA played a negligible role in our experiments.

5. Conclusions

Contrary to widespread assumption that chemical processes are likely the dominant source of nitrite scavenging under acidic conditions (Dail et al., 2001; McKenney et al., 1990; Nömmik and Thorin, 1972; Yamulki et al., 1997), we have provided strong evidence for biologically-driven control of nitrite levels in acidic environments during denitrification. However, abiotic nitrite decomposition did play a role, and the competition between the two nitrite sinks (nitrite reductase and abiotic transformations) has implications for the ultimate fate of nitrate-N: at low and intermediate pH, abiotic nitrite transformations resulted in conversion of a significant fraction (10-20 %) of nitrite-N to nitroso-compounds. This underscores the need to take the abiotic nitrite kinetics into account in studies of biological nitrogen redox transformations in soils with pH $\leq$ 5.

Acknowledgements

The authors thank Bioforsk Vest Fureneset for providing the Fjaler soils, and Heidi Hillier (MSc student in KBM, NMBU) for sample collection and assisting in laboratory work.

Supplementary material to Lim *et al.*

Content:

S1. Comparison of sterilisation methods

Removing all bioactivity from the soils is necessary to determine the kinetics of abiotic decomposition of N-oxyanions (NO_3^- and NO_2^-). To determine the most suitable way to sterilise the soils with minimal effects on the soil chemistry, three sterilisation methods were tested on soils L and H. The methods were chosen based on their historical and/or frequent use in the literature (Labeda et al., 1975; Silva Aquino, 2012; Trevors, 1996; Tuominen et al., 1994).

Autoclaving: Soil (10 g fw) was measured into pre-weighed 120 mL serum vials, covered with aluminium foil, then autoclaved for 15 min at 121 °C and 15 psi. The extra moisture in the vials post-autoclaving (condensation water) was removed by drying in a 50 °C oven until the vials reached the original weight. The aluminium foil covers were removed and the vials were sealed with pre-sterilised air-tight rubber septa and aluminium crimps in a class II biosafety cabinet.

Chloroform fumigation: Soil was transferred to disposable aluminium specimen containers, and kept to less than 5 cm in depth to ensure effective transport of chloroform into the soil matrix. The chloroform was water-washed to remove ethanol (the stabilising agent in chloroform), and transferred to a large glass evaporation dish with glass beads and boiling chips, then placed in the lower compartment of a chemical-resistant glass vacuum desiccator. The soil samples were placed on the perforated porcelain plate in the desiccator, which was then evacuated until the chloroform boiled, then kept under vacuum for 1 min before venting to laboratory air. This evacuation procedure was repeated three times, then the chamber was left sealed with a chloroform atmosphere for 24 h. The chloroform was then removed from the desiccator, and the soil was rinsed by evacuation and venting the chamber to laboratory air 15 times. The samples were left to laboratory air for 24 h before repeating the chloroform fumigation again. This "fumigation and air-exposed" procedure was repeated thrice. During the final air-exposure process, the samples were left on a laminar-air flow bench for 1.5 h to evaporate any residual chloroform left in the soil prior to transferring to glass vials and sealed with septa and crimps.

Gamma irradiation: Soil samples were given a dose of 27.8 kGy (^{60}Co) (at the Institute of Energy Technology, Kjeller, Norway). The gamma-irradiated soil was stored for 3 months at 4 °C before use, to deplete free radicals generated by radiolysis.

The success of each sterilisation method was tested by incubating soils with filter-sterilised $NaNO_2$ (0.5 μmol g^{-1} soil fw), with and without glutamate (2.5 μmol g^{-1} soil fw), to aid in the detection of metabolic activity. The sterilised soils (10 g fw) were placed in 120 mL serum vials, the air replaced with He (to enable the detection of denitrification products) or He+1 vol% O_2 (for measuring O_2 consumption and CO_2 production). The O_2 consumption, CO_2 production, denitrification and/or chemodenitrification rates were monitored for 5 days. A water bath and thermostat kept the samples at 15 °C. The evolution and consumption of gases were monitored using a robotised auto-sampling and incubation system (Molstad et al., 2007). Headspace gases were sampled and measured automatically every 3-5 h by the system using a gas chromatograph and NO analyser: CO_2 and O_2 were monitored for respiratory activity, whereas NO, N_2O and N_2 gases were used to determine denitrification activity and abiotic NO_2^- decomposition to NO and N_2O. The amounts of NO and N_2O are either reported as measured (mol $vial^{-1}$), or as cumulated production, which is the measured amounts corrected for the losses by sampling (see Molstad et al., 2007).

Immediately following the oxic incubation, the numbers of viable organisms in the sterilised soils were determined by dilution plating on one-tenth (10 %) strength tryptic soy agar (TSA, Difco) with cycloheximide (100 μg/mL), and on malt agar (MA, Sigma-Aldrich) with streptomycin (100 μg/mL), to enumerate bacteria and fungi, respectively. The soils were dispersed in sterile water (1:4, w/w) by vigorous shaking and allowed to settle for ≈5 min before the supernatant was diluted and plated on agar, using both pour- and spread-plate techniques. The plates were incubated 15 °C for 4 days, and colony numbers were recorded daily.

Autoclaving and gamma-irradiation effectively sterilised both soils (H, and L), as evidenced by the absence of colony-forming bacteria (plate counting, results not shown) and extremely low oxygen consumption rates which were not enhanced by adding glutamate; tested 2 months after sterilisation. In the gamma-irradiated soils L, M and H incubated without glutamate, the oxygen consumption rates (μmol g^{-1} dw h^{-1}) were 0.018 (0.003), 0.24 (0.016) and 0.35 (0.028), respectively (standard error in parenthesis), and very similar and stable rates were recorded when incubated with glutamate.

Chloroform fumigation effectively eliminated aerobic respiration in soil L for the entire incubation period (immediately after sterilisation), but in soil H the effect was transient: respiration was practically zero during the first 20 h, and then increased exponentially. Thus, autoclaving and gamma-irradiation were the only methods that permanently eliminated microbial activity in both soils, while chloroform fumigation had a transient effect: the metabolic activity was effectively close to zero only during the first 20 h.

To further evaluate the effect of the sterilisation methods, we incubated soil anaerobically with glutamate and nitrite. The NO production during anaerobic incubations of sterilised soils to which nitrite was injected are shown in Fig. S1. Soil L (pH 3.4) showed rapid accumulation of NO reaching 900-1000 nmol $vial^{-1}$ during the first 1-2 h of anaerobic incubation for both the gamma-irradiated and chloroform-fumigated soils. The gradual decline thereafter is due to autoxidation (Nadeem et al. 2013). In comparison, the NO production by the autoclaved soil L was only ≈15 % of that in the chloroform fumigated and gamma-irradiated soil L (Fig. 1). For soil H, practically no NO was produced in any of the sterilised samples, except for a sudden burst in NO from the chloroform fumigated soil after ≈35 h. The latter was ascribed to the escalating metabolism in the chloroform fumigated soil, starting around 20 h after incubation (in the aerobic incubation used to test sterility, see above).

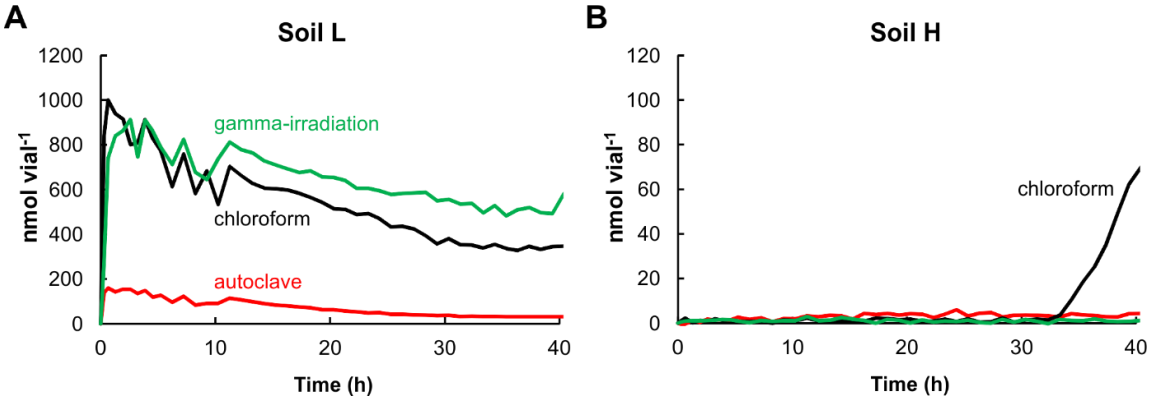

Fig. S1 *Production of NO (nmol per vial) in autoclaved (red), chloroform-fumigated (black) and gamma-irradiated (green) soils incubated with glutamate and nitrite at 1 vol% O_2 in headspace.* ***A)*** *soil L (pH 3.4),* ***B)*** *soil H (pH 7.1).*

Our purpose with soil sterilisation was to assess the kinetics of abiotic nitrite decomposition to NO (and possibly N_2O and N_2), and the results shown in Fig. S1 were taken to indicate that gamma irradiation was preferred over autoclaving, based on the following reasoning: None of the sterilisation techniques will leave the soil matrix unaffected (physically and chemically), thus there is a risk of biased assessment of the nitrite decay with any of the methods. However, chloroform fumigation had perceivably the least impact (compared to autoclaving and gamma sterilisation). The gamma-irradiated and chloroform fumigated soils showed practically identical NO kinetics in soil L, while autoclaved soil produced miniscule amounts of NO. We therefore assume that gamma irradiation had a less severe effect on relevant physical and chemical properties compared to autoclaving, which is known to induce quite profound changes both of structure and chemistry, as reviewed by Trevors (1996).

In summary, gamma-irradiation was the only of the four methods that was able to suppress microbial respiration in both soils L and H, and which had an apparent marginal interference with the abiotic nitrite decomposition. Additionally, soil pH was only marginally lowered by gamma-irradiation (3.44→3.40, 5.54→4.90, 7.24→7.06). Thus, gamma-irradiation was used to sterilise soils in all experiments presented in the main article.

S2. Nitrite recovery by rapid extraction in water

The kinetics of anion exchange was investigated by rapid water extraction at time intervals during the first 10 min after addition of nitrite to soils (10 mL of 10 mM KNO_2, added to 0.2 g soil fresh weight). The result is shown in Fig. S2, together with modelled kinetics according to equation S1

$$\frac{dNO_{2\,w}^{-}}{dt} = -k \cdot (NO_{2w} - NO_{2S} \cdot R) \qquad \text{(S1)}$$

where NO_{2w} is "free nitrite", NO_{2s} is adsorbed nitrite, k is the rate constant (min^{-1}) and R is the ratio NO_{2w}/ NO_{2s} at equilibrium.

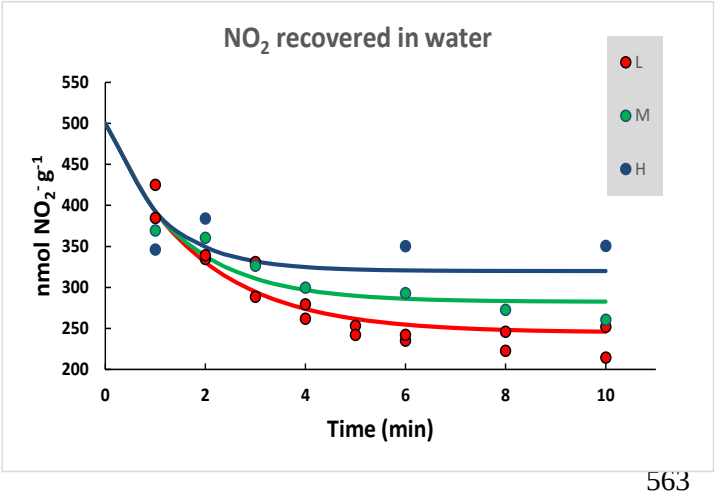

Fig. S2 *Short term equilibration of nitrite by ion exchange with the soil matrix. The figure shows the measured nitrite (nmol g^{-1} soil fresh weight) in the supernatant after rapid extraction in microcentrifuge tubes (centrifuged immediately after vortexing for 10-15 sec), at time intervals after adding 500 nmol g^{-1} fresh weight (% dry weight was 25, 42 and 43 for soil L, M and H respectively) The curves show predicted values, assuming R = 0.96, 1.32 and 1.78 for the soils with pH 3.4, 4.9 and 7, respectively, and k = 0.21 min^{-1}. P is the fraction of adsorbed NO_2^- at equilibrium and k is the transfer coefficient; as defined by equation S1. The fraction of total nitrite at equilibrium is R/(1+R).*

To further elucidate the effect of ion exchange and to determine the exact partitioning at equilibrium, two types of experiments were conducted. First, nitrate was used as a surrogate for nitrite, and the efficiency of water extraction was evaluated by comparing with nitrate extracted by 2 M KCl. Table S1 summarises the recovery in water extracts compared to KCl. It shows a low recovery for the water extraction, confirming that anion exchange is significant.

574 ***Table S1*** *Nitrate extracted by the rapid water extraction procedure compared to extraction with 2 M KCl. Standard*
575 *error is shown in parenthesis (n=4-6).*

Soil	NO_3^- in solution, µmol g^{-1}	
	2 M KCl	**MilliQ water**
L	11.1 (0.6)	6.9 (0.3)
H	13.9 (0.2)	9.5 (0.6)

576

577 The fraction of nitrite extracted by water is theoretically affected by the total amount of nitrite
578 present; it is expected to increase when nitrite concentrations approach the anion exchange capacity of
579 the soil. To inspect this, we added a range of nitrite concentrations to two of the soils (gamma-irradiated
580 soil L and H), and performed water extractions 10 min after addition. The measured nitrite in the water
581 is shown in Fig. S2, plotted against the added amounts of nitrite.

582

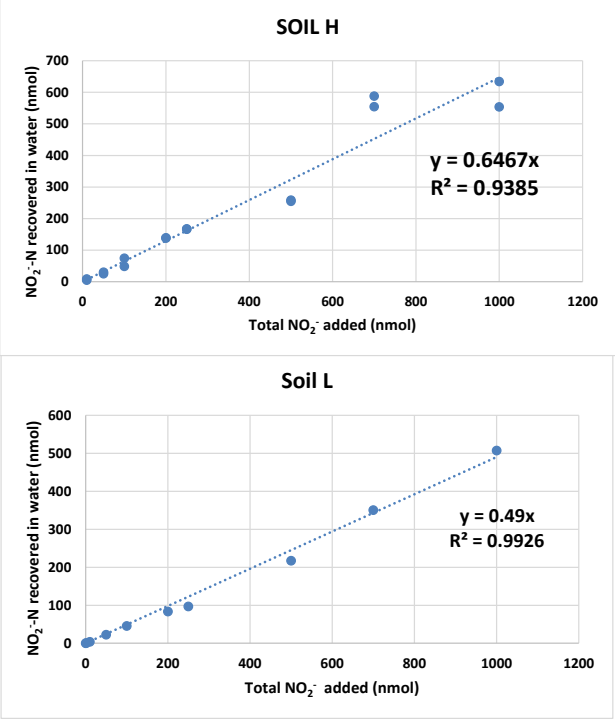

Fig. S3 *Recovery of added NO_2^- by rapid water extraction, 10 min after addition. Experiment conducted in microcentrifuge tubes containing 0.2 g fresh weight soil [25% dry weight for soil L (pH 3.4) and 40 % dry weight for soil H (pH7.1)] to which 10 µL of KNO_2 (concentration range 1-100 mM) was added. Nitrite was extracted with 0.5 mL distilled water. Linear regression functions are shown; the regression coefficients estimating the fraction of total NO_2^- extracted, F = 0.49 for soil L and 0.65 for soil L. An intermediate value of F = 0.57 was assumed for the soil with intermediate pH (soil M). These values were used for the simulation of the kinetics shown in Fig. S1 (R in equation 1 is equal to F/(1-F)).*

598

599

S3. Nitrite decay

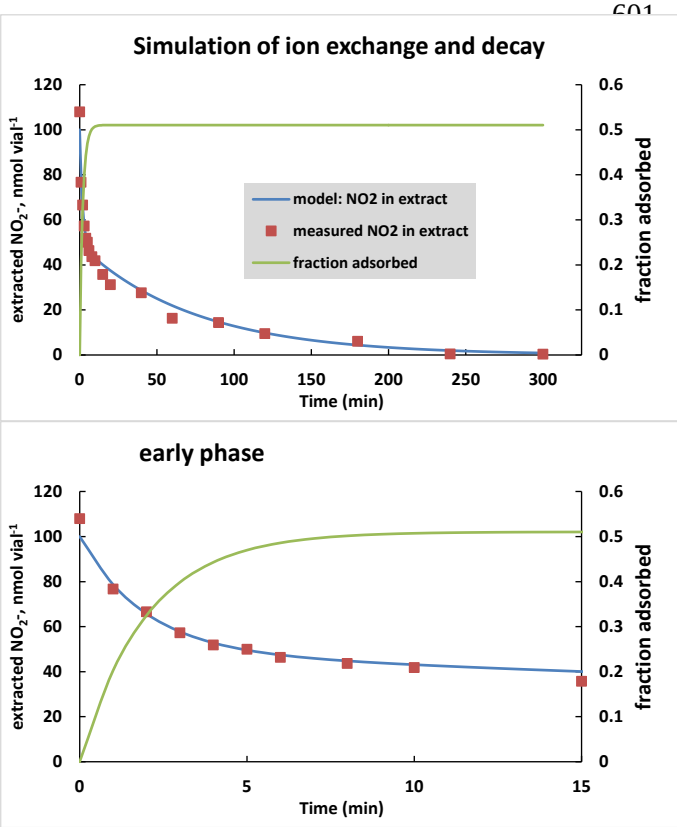

Fig. S4 *Simulation of ion exchange and decay during the 0-5 h oxic experiment with soil L. The panel shows measured nitrite in water extract (nmol vial^{-1}), and the simulation of the kinetics of nitrite in water extracts based on the combined kinetics of ion exchange (Fig. S1) and first order nitrite decay. The ion exchange rate is given by equation S1. The decay rate is assumed to be first order with respect to total NO_2^-; $d(NO_{2w}+NO_{2s})/dt=-k(NO_{2w}+NO_{2s})$. The green line shows fraction of total NO_2^- adsorbed; i.e. 1/(1+R) (equation S1). The model was fitted to data, and the parameter values are t = 0.2 min^{-1} and k = 0.013 min^{-1}, equivalent to 0.78 h^{-1} , which is slightly higher than that determined for anoxic incubations of the same soil (0.73 h^{-1}; Fig. S5).*

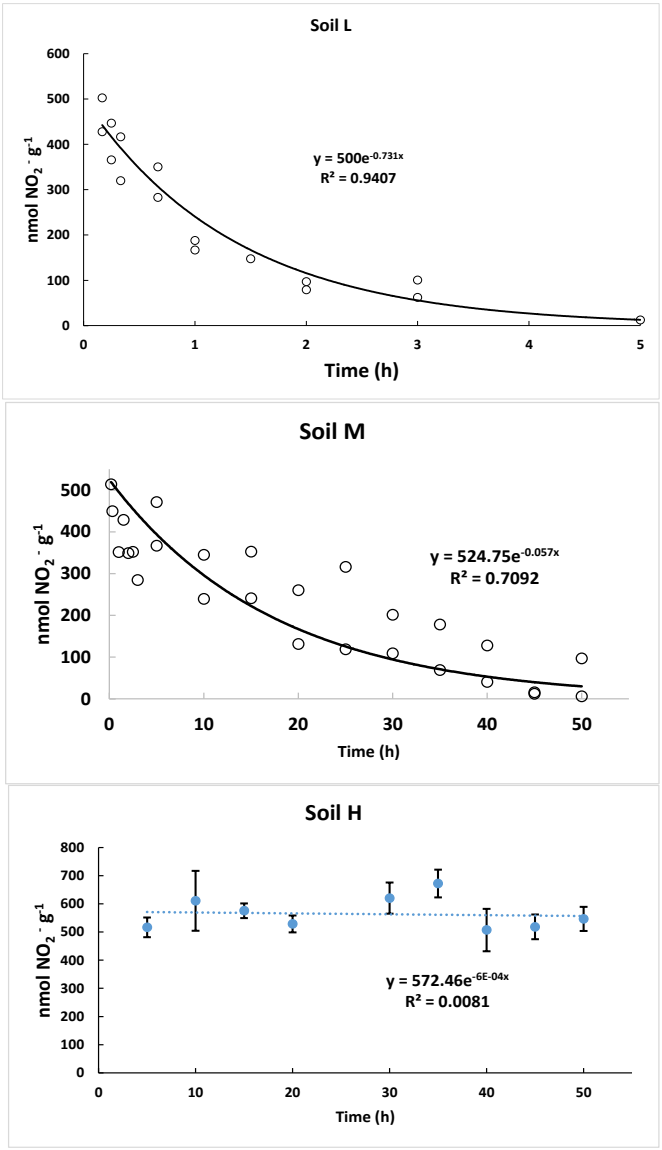

Fig. S5 *Nitrite decay during anoxic incubations of gamma-irradiated soils. The panels show residual nitrite (nmol NO_2^- g^{-1} fresh weight soil against time. The top panel shows the result for the 0-5 h experiment with soil L, excluding the data for the first 10 min (due to lack of equilibration between adsorbed and extractable nitrite, see Fig. S1). The lower two panels show the results for soil M and H. Single measurements are shown for soil L and M, and average for 4 replicates are shown for soil H. First order decay functions fitted to data are shown for each soils. Residual nitrite is calculated from measured nitrite in water (fast extraction), corrected for the fraction of extractable nitrite for each soil (see Fig. S2). Estimated decay rates constants (h^{-1}) for each soil are:*

Soil L: 0.73 h^{-1} (SE: 0.065)

Soil M: 0.057 h^{-1} (SE: 0.007)

Soil H: 0.00055 h^{-1} (SE: 0.002)

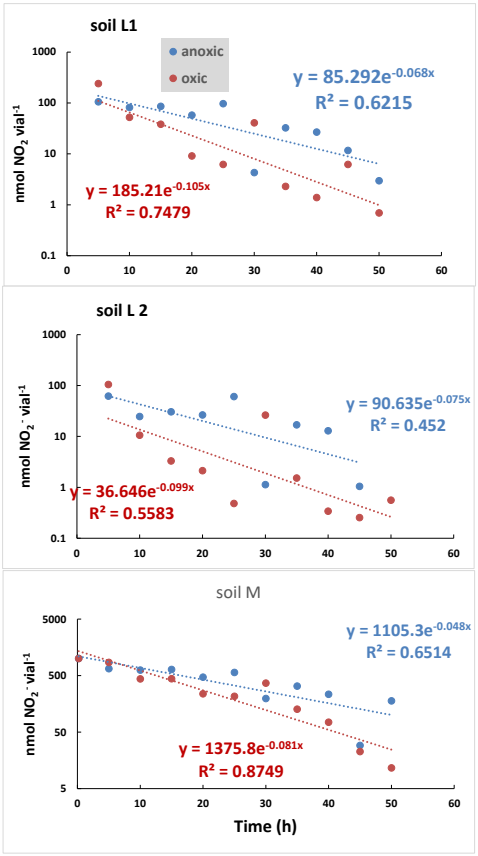

Fig. S6 Comparison of aerobic and anaerobic nitrite decay in gamma-irradiated soils. *2 g soil (fresh weight) was incubated in 12 mL vials crimp sealed with butyl rubber septa. One set was kept aerobic, the other was anaerobised (replaced atmosphere with He) prior to injection of nitrite (*spreading 0.1 mL 10 mM KNO_2 *onto the surface). At time intervals, vials were sacrificed to measure residual nitrate. The panels show the result for three soils (2 replicates of soil L and one for M), and the fitted exponential functions.*

652

653

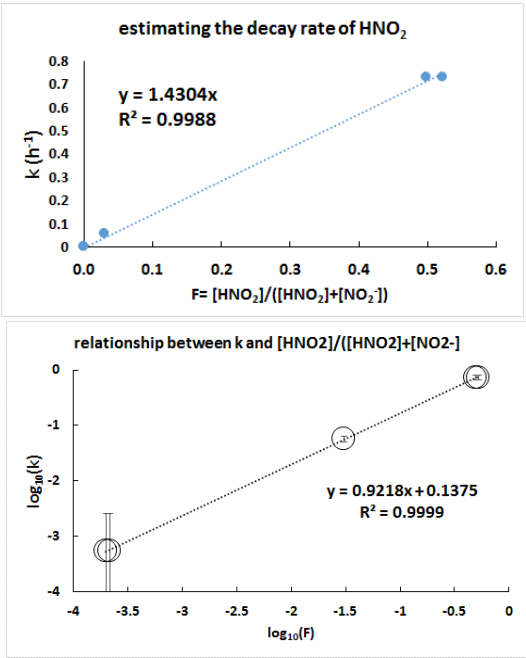

Fig. S7 *Relationship between un-dissociated HNO_2 and observed decay rates of total nitrite (TONI=NO_2^-+HNO_2) in the three soils. The two panels show the estimated first order decay rates of nitrite (i.e. NO_2^-+HNO_2) plotted against the fraction of un-dissociated HNO_2. Top panel is a linear plot, the lower panels shows a log-log plot. The regression function in the top plot effectively estimates the first order decay rate of un-dissociated HNO_2 in the soils (k_{HNO2} = 1.43 h^{-1}, since we assume that $d[TONI]/dt=[TONI]*F*k_{HNO2}$). The regression function for the lower plot should in theory be $y=log_{10}(F*k_{HNO2}) = log_{10}(F)+ log_{10}(k_{HNO2})$, thus the estimated k_{HNO2} is $10^{0.1375}$ = 1.37 h^{-1}. The estimates are surprisingly similar to the aerobic rates of nitrite decay (oxidation rates of HNO_2 in water) determined by Braida and Ong (1999).*

668

669 ***Table S2*** *Measured N_2-N production (µmol vial^{-1}); cumulated production during the entire 135 hour anaerobic*
670 *incubation of gamma-irradiated soils, with and without 2.5 µmol NO_2^- vial^{-1} (=1 µmol g^{-1} soil fresh weight; soil*
671 *moisture = 50% w/w). The average values for three replicate vials of each soil are shown, with standard deviation.*
672 *The last column (Δ) shows the difference between vials with and without NO_2^-.*

	with NO_2^-		**Control**		Δ
	avg	**stdev**	**avg**	**stdev**	
Low pH	0.04	0.12	0.20	0.13	-0.15
Mid pH	0.23	0.24	0.31	0.29	-0.08
High pH	-0.15	0.22	0.17	0.10	-0.31

673

674

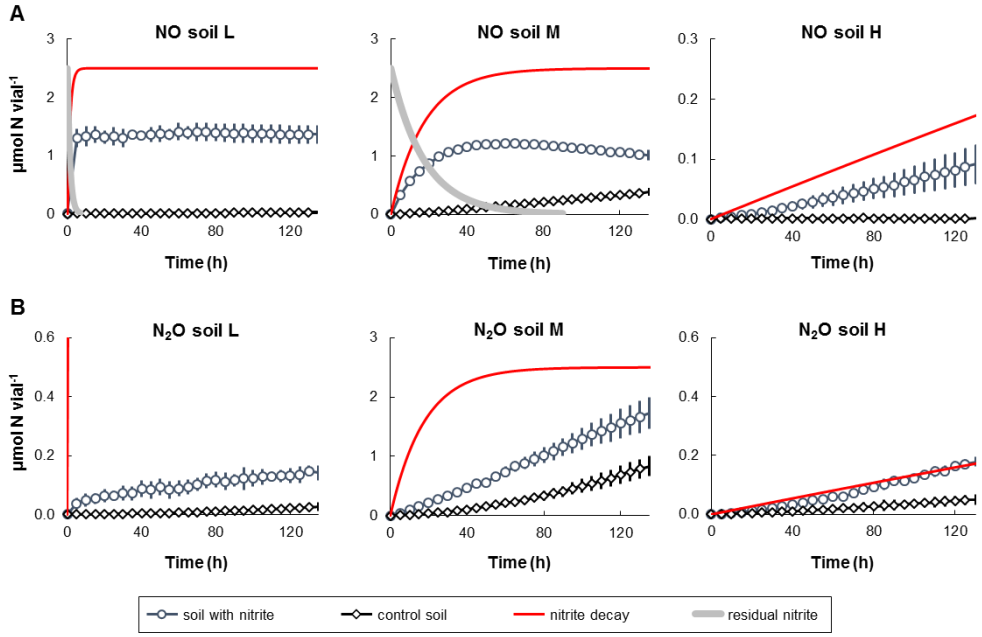

Fig. S8 *NO production by NO_2^- decay in gamma-irradiated soil during anoxic incubation (2.5 µmol $NaNO_2$ was added to 5 g soil fresh weight). Entire incubation shown for all soils (equivalent to Fig. 2 in the main paper). The panels show cumulated production of NO (panel A) and N_2O (panel B) in control soil (no nitrite added) and in nitrite amended soil (2.5 µmol NO_2 to 10 g soil fresh weight in each vial). The residual nitrite, as predicted by the first order decay is shown as grey curves (not shown for soil H due to scaling). The red curves show the cumulated nitrite decay. The decline in NO in soil M after 50 h is due to neither sampling nor autoxidation.*

References:

Braida W, Ong SK,(2000) Decomposition of nitrite under various pH and aeration conditions. Water, Air and Soil Pollution 118:13-26

Labeda, D.P., Balkwill, D.L., Casida Jr., L.E., 1975. Soil sterilization effects on *in situ* indigenous microbial cells in soil. Canadian Journal of Microbiology 21, 263–269.

Silva Aquino, K.A. da, 2012. Sterilization by Gamma Irradiation, in: Gamma Radiation. InTech. doi:10.5772/34901

Trevors, J.T., 1996. Sterilization and inhibition of microbial activity in soil. Journal of Microbiological Methods 26, 53–59. doi:10.1016/0167-7012(96)00843-3

Tuominen, L., Kairesalo, T., Hartikainen, H., 1994. Comparison of methods for inhibiting bacterial activity in sediment. Applied and Environmental Microbiology 60, 3454–7.

References

Bancroft, K., Grant, I.F., Alexander, M., 1979. Toxicity of NO2: Effect of Nitrite on Microbial Activity in an Acid Soil. Appl. Envir. Microbiol. 38, 940–944.

Braman, R.S., Hendrix, S.A., 1989. Nanogram nitrite and nitrate determination in environmental and biological materials by vanadium(III) reduction with chemiluminescence detection. Analytical Chemistry 61, 2715–2718. doi:10.1021/ac00199a007

Breuillin-Sessons, F., Ventera, R.T., Sadowsky, M.J., Coulter, J.A., Clough, T.J., Wang, P. 2017. Nitrification gene ratio and free ammonia explain nitrite and nitrous oxide productin in urea-amended soils. Soil Biology and Biochemistry 111:143-153.

Colman, B.P., Fierer, N., Schimmel, J.P. 2007. Abiotic nitrate incorporation in soil: is it real? Biogeochemistry 84:161-169.

Cox, R.D., 1980. Determination of nitrate and nitrite at the parts per billion level by chemiluminescence. Analytical Chemistry 52, 332–335. doi:10.1021/ac50052a028

Dail, D.B., Davidson, E.A., Chorover, J., 2001. Rapid abiotic transformation of nitrate in an acid forest soil. Biogeochemistry 54, 131–146. doi:10.1023/A:1010627431722

Glass, C., Silverstein, J., 1998. Denitrification kinetics of high nitrate concentration water: pH effect on inhibition and nitrite accumulation. Water Research 32, 831–839. doi:10.1016/S0043-1354(97)00260-1

Heil, J. Verecken, H., Brüggemann, N. 2016. A review of chemical reactions of nitrification intermediates and their role in nitrogen cycling and nitrogen trace gas formation in soil. European Journal of Soil Science 67:23-39.

Homyak, P.M., Vasquez, K.T., Sickman, J.O., Parker, D.R., Schimel, J.P., 2015. Improving Nitrite Analysis in Soils: Drawbacks of the Conventional 2 M KCl Extraction. Soil Science Society of America Journal 79, 1237–1242. doi:10.2136/sssaj2015.02.0061n

Jacob, D.J., 2000. Heterogeneous chemistry and tropospheric ozone. Atmospheric Environment 34, 2131–2159. doi:10.1016/S1352-2310(99)00462-8

Kaiser, G., Heber, U., 1983. Photosynthesis of leaf cell protoplasts and permeability of the plasmalemma to some solutes. Planta 157, 462–470. doi:10.1007/BF00397204

Kulmala, M., Petäjä, T., 2011. Soil Nitrites Influence Atmospheric Chemistry. Science 333, 1586–1587. doi:10.1126/science.1211872

Liu, B., Frostegård, Å., Bakken, L.R., 2014. Impaired reduction of N2O to N2 in acid soils is due to a posttranscriptional interference with the expression of nosZ. mBio 5, e01383-14. doi:10.1128/mBio.01383-14

Liu, B., Mao, Y., Bergaust, L., Bakken, L.R., Frostegård, Å., 2013. Strains in the genus Thauera exhibit remarkably different denitrification regulatory phenotypes. Environmental Microbiology n/a-n/a. doi:10.1111/1462-2920.12142

Liu, B., Mørkved, P.T., Frostegård, Å., Bakken, L.R., 2010. Denitrification gene pools, transcription and kinetics of NO, N2O and N2 production as affected by soil pH. FEMS Microbiology Ecology 72, 407–417. doi:10.1111/j.1574-6941.2010.00856.x

Lycus, P., Bøthun, K.L., Bergaust, L., Shapleigh, J.P., Bakken, L.R., Frostegård, Å. 2017. Phenotypic and genotypic richness of denitrifiers revealed by a novel isolation strategy. The ISME Journal 11:2219-2232.

Mania, D., Heylen, K., van Spanning, R.J.M., Frostegård, Å., 2014. The nitrate-ammonifying and nosZ -carrying bacterium Bacillus vireti is a potent source and sink for nitric and nitrous oxide under high nitrate conditions. Environmental Microbiology 16, 3196–3210. doi:10.1111/1462-2920.12478

McKenney, D.J., Lazar, C., Findlay, W.J., 1990. Kinetics of the Nitrite to Nitric Oxide Reaction in Peat. Soil Science Society of America Journal 54, 106. doi:10.2136/sssaj1990.03615995005400010016x

Molstad, L., Dörsch, P., Bakken, L.R., 2007. Robotized incubation system for monitoring gases (O_2, NO, N_2O, N_2) in denitrifying cultures. Journal of Microbiological Methods 71, 202–211. doi:http://dx.doi.org/10.1016/j.mimet.2007.08.011

Molstad, L, Dörsch, P., Bakken, L.R. (2016) Improved robotized incubation system for gas kinetics in batch cultures. Researchgate 308118692 , DOI: 10.13140/RG.2.2.30688.07680

Nömmik, H., Thorin, J., 1972. Transformations of 15N-labelled nitrite and nitrate in forest raw humus during anaerobic incubation, in: IAEA (Ed.), Isotopes and Radiation in Soil Plant Relationships Including Forestry. IAEA-SM-151/58, Vienna, Austria, pp. 369–382.

Qu, Z., Bakken, L.R., Molstad, L., Frostegård, Å., Bergaust, L.L., 2016. Transcriptional and metabolic regulation of denitrification in *Paracoccus denitrificans* allows low but significant activity of nitrous oxide reductase under oxic conditions. Environmental Microbiology 18, 2951–2963. doi:10.1111/1462-2920.13128

Samouilov, A., Woldman, Y.Y., Zweier, J.L., Khramtsov, V.V., 2007. Magnetic resonance study of the transmembrane nitrite diffusion. Nitric Oxide 16, 362–370. doi:10.1016/j.niox.2006.12.006

Shen, Q., Ran, W., Cao, Z.., 2003. Mechanisms of nitrite accumulation occurring in soil nitrification. Chemosphere 50, 747–753. doi:10.1016/S0045-6535(02)00215-1

Sognnes, L.S., Fystro, G., Øpstad, S.L., Arstein, A., Børresen, T., 2006. Effects of adding moraine soil or shell sand into peat soil on physical properties and grass yield in western Norway. Acta Agriculturae Scandinavica, Section B - Soil & Plant Science 56, 161–170. doi:10.1080/09064710500218845

Spott, O., Russow, R., Stange, C.F., 2011. Formation of hybrid N2O and hybrid N2 due to codenitrification: First review of a barely considered process of microbially mediated N-nitrosation. Soil Biology and Biochemistry 43, 1995–2011. doi:10.1016/j.soilbio.2011.06.014

Stevens, R.J., Laughlin, R.J., Malone, J.P., 1998. Soil pH affects the processes reducing nitrate to nitrous oxide and di-nitrogen. Soil Biology and Biochemistry 30, 1119–1126. doi:10.1016/S0038-0717(97)00227-7

Su, H., Cheng, Y., Oswald, R., Behrendt, T., Trebs, I., Meixner, F.X., Andreae, M.O., Cheng, P., Zhang, Y., Pöschl, U., 2011. Soil nitrite as a source of atmospheric HONO and OH radicals. Science (New York, N.Y.) 333, 1616–8. doi:10.1126/science.1207687

Van Cleemput, O., Samater, A.H., 1996. Nitrite in soils: accumulation and role in the formation of gaseous N compounds. Fertilizer Research 45, 81–89. doi:10.1007/BF00749884

Van Spanning, R.J.M., Richardson, D.J., Ferguson, S. 2007. Introduction to the biochemistry and molecular biology of denitrification. p 3-21 in: Bothe H, Ferguson S, Newton WE (eds) The biology of the Nitrogen cycle. Elsevier (Amsterdam) ISBN-13: 978-0-444-52857-5.

788 Ventera, R.T., Rolston, D.E. (2000a) Mechanisms and kinetics of nitric and nitrous oxide
789 production during nitrification in agricultural soil. Global Change Biology 6, 303-
790 316.

791 Ventera, R.T., Rolston, D.E. (2000b) Nitric and nitrous oxide emissions following
792 fertilizer application to agricultural soil: Biotic and abiotic mechanisms and
793 kinetics. Journal of Geophysical Research 105, 15117-15129.

794 Ventera, R.T., Rolston, D.E., Cardon, Z.G. (2005) Effects of soil moisture, physical, and
795 chemical characteristics on abiotic nitric oxide production. Nutrient Cycling in
796 agroecosystems 72, 27-40. DOI 10.1007/s10705-004-7351-5

797 Ventera, R.T., Clough, Y.J., Coulter, J.A., Breuillin-Sessoms, F. 2015. Ammonium
798 sorption and ammonia inhibition of nitrite-oxidizing bacteria explain contrasting
799 soil N_2O production. Scientific Reports 5:12153, DOI: 10.1038/srep12153.

800 Yamulki, S., Harrison, R.M., Goulding, K.W.T., Webster, C.P., 1997. N2O, NO and NO2 fluxes
801 from a grassland: Effect of soil pH. Soil Biology and Biochemistry 29, 1199–1208.
802 doi:10.1016/S0038-0717(97)00032-1

803 Yoon, S., Cruz-García, C., Sanford, R., Ritalahti, K.M., Löffler, F.E., 2015. Denitrification
804 versus respiratory ammonification: environmental controls of two competing
805 dissimilatory NO3−/NO2− reduction pathways in Shewanella loihica strain PV-4.
806 The ISME Journal 9, 1093–1104. doi:10.1038/ismej.2014.201

807 Zhang, J., Lan, T., Müller, C., Cai, Z., 2015. Dissimilatory nitrate reduction to ammonium
808 (DNRA) plays an important role in soil nitrogen conservation in neutral and alkaline
809 but not acidic rice soil. Journal of Soils and Sediments 15, 523–531.
810 doi:10.1007/s11368-014-1037-7

811 Zhu-Barker, X., Cavazos, A.R., Ostrom, N.E., Horwath, W.R., Glass, J.B., 2015. The
812 importance of abiotic reactions for nitrous oxide production. Biogeochemistry 126,
813 251–267. doi:10.1007/s10533-015-0166-4

814

Tables and figures

Table 1. Decay rate of NO_2^- in gamma-irradiated soils under anoxic conditions. The table shows soil pH, the partitioning of nitrite ions during water extraction, R = estimated ratio between NO_2^- in the distilled water and NO_2^- adsorbed to soil particles after extraction with distilled water, WF = fraction of NO_2^- in the water (=R/(R+1)), and k_d = the estimated first order decay rate constant (h^{-1}) under anoxic conditions (standard error in parenthesis)

Lime treatment	pH	R	WF	k_d (h^{-1})
L	3.44	0.77	0.44	0.73 (0.065)
M	4.90	0.74	0.43	0.057 (0.007)
H	7.24	1.37	0.58	0.00055 (0.002)*

** the decay rate for soil H is not significantly different from zero.*

Table 2. Nitrate N mass balance. The table shows the recovery of NO_3^- -N as N gases (NO, N_2O and N_2) and as R-NO (abiotic reactions with soil organic matter, Fig. 2). The bottom row shows the total recovery (% of NO_3^--N in parenthesis).

	Soil L	Soil M	Soil H
Initial NO_3	37.0	40.0	26.0
N_2	24.5	32.0	25.0
Sampling loss[1]	4.1	2.0	1.1
N-gas, total	**28.6**	**34.0**	**26.1**
R-NO[2]	14*0.45 = 6.3	17*0.4 = 6.8	0.14*0.4 = 0.06
N accounted for (%)	**34.9 (94 %)**	**40.8 (102 %)**	**26.2 (101 %)**

[1] The cumulative N_2 as estimated (Fig 3) includes the sampling loss of N_2, but not the loss of NO and N_2O. To estimate the total amount of N-gas, the cumulative sampling loss of N_2O and NO were added.

2 The amount of nitrosated soil organic matter (R-NO) produced, estimated as the product of the cumulative abiotic nitrite reaction (V_{ADEC}) and the R-NO-fraction (=1-f_{NO}-f_{N2O}) observed in gamma-sterilized soil (see text for further details).

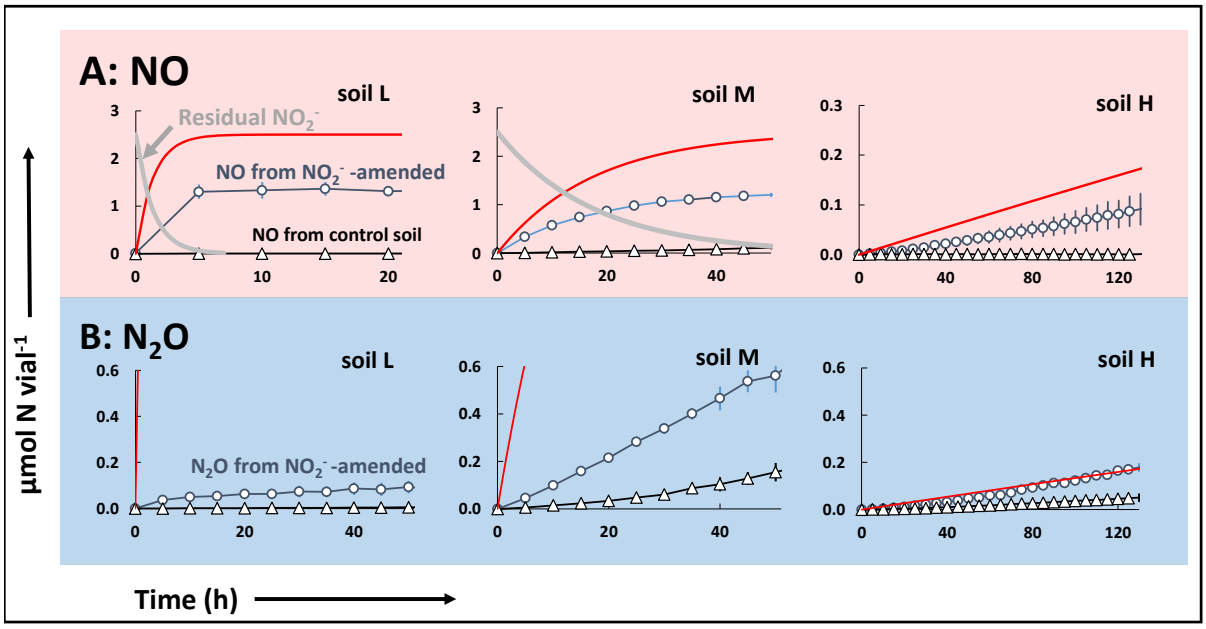

Fig. 1. Nitrite (NO_2^-) decay, NO and N_2O production in gamma-irradiated soil L (pH 3.4), M (pH 4.9) and H (pH 7.1). The panels show cumulative production of NO (**A**) and N_2O (**B**) in in nitrite amended soil (2.5 µmol NO_2 to 10 g soil fw in each vial). The residual nitrite, as predicted by the first order decay is shown as grey curves, and the red curves show the cumulative nitrite decay. Residual nitrite in soil H remained high throughout (Fig. S5), and is not visible due to scaling. For comparison, the NO- and N_2O-production in control soils (no nitrite added) are shown as triangles (◊) Note that the scales are different and only the first part is reported for soil M and L to enhance visibility. Results for the entire incubation for all soils is found in Supplementary Fig. S8.

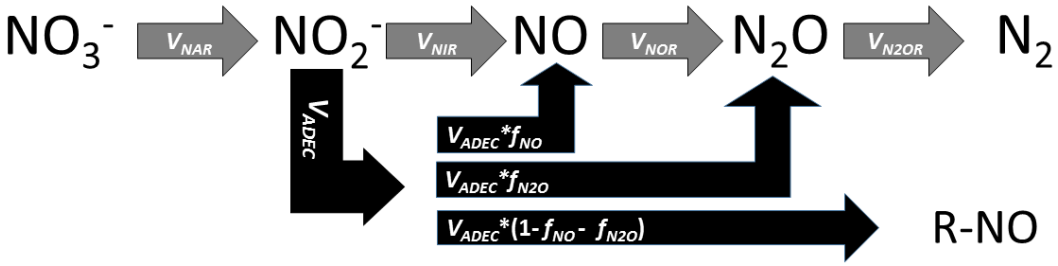

Fig. 2. Calculations of enzymatic and abiotic transformations. Enzymatic transformations are denoted by grey arrows. Abiotic transformations (black arrows) were estimated based on measured concentrations of nitrite, the first order decay, and partitioning, as observed in gamma-irradiated soils. This allowed the estimation of enzymatic reduction rates based on the measured rates of change in NO_2^-, NO, N_2O and N_2 (equations 2-7). V_{NAR}, V_{NIR}, V_{NOR}, and V_{N2OR} are the rates of enzyme-mediated reactions. V_{ADEC} is the predicted rate of abiotic nitrite decomposition. R-NO is the nitrosated/nitrosylated organic compounds.

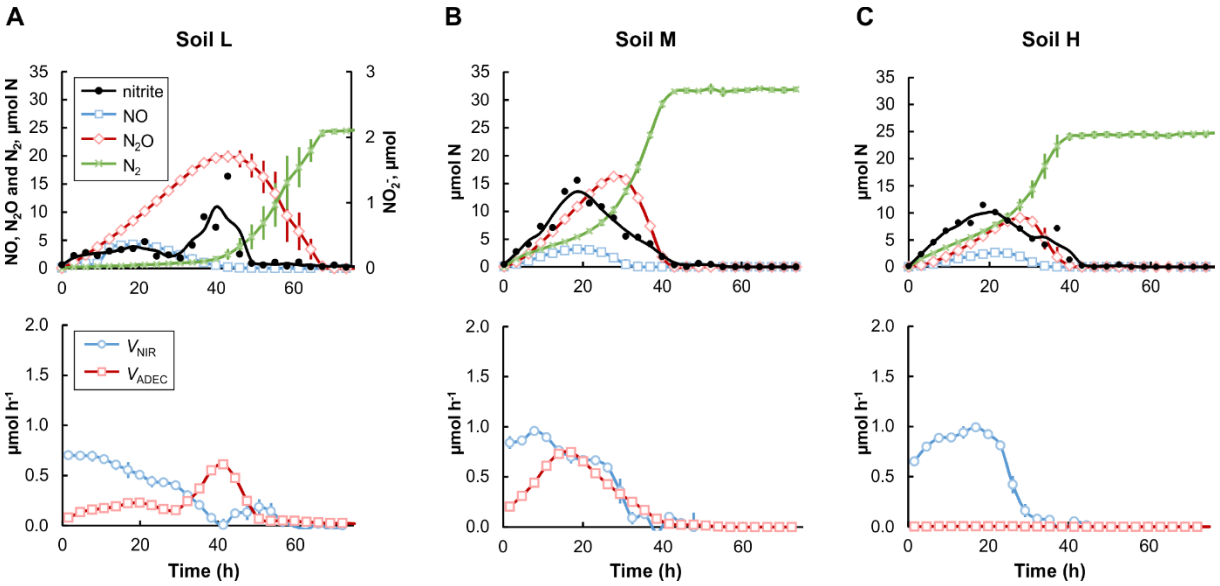

Fig. 3. Kinetics of denitrification and evaluation of abiotic NO_2^- decomposition versus enzymatic reduction of NO_2^-. Top panels show the measured NO_2^- (single measurements and floating average as black circles and lines, respectively), together with measured NO and N_2O and cumulative N_2 production (i.e. corrected for dilution by sampling), and are averages of three replicate vials (standard deviation as vertical lines). The lower panels show the estimated rates of enzymatic nitrite reduction (V_{NIR}) and the rate of abiotic nitrite decomposition (V_{ADEC}); see text for explanation.

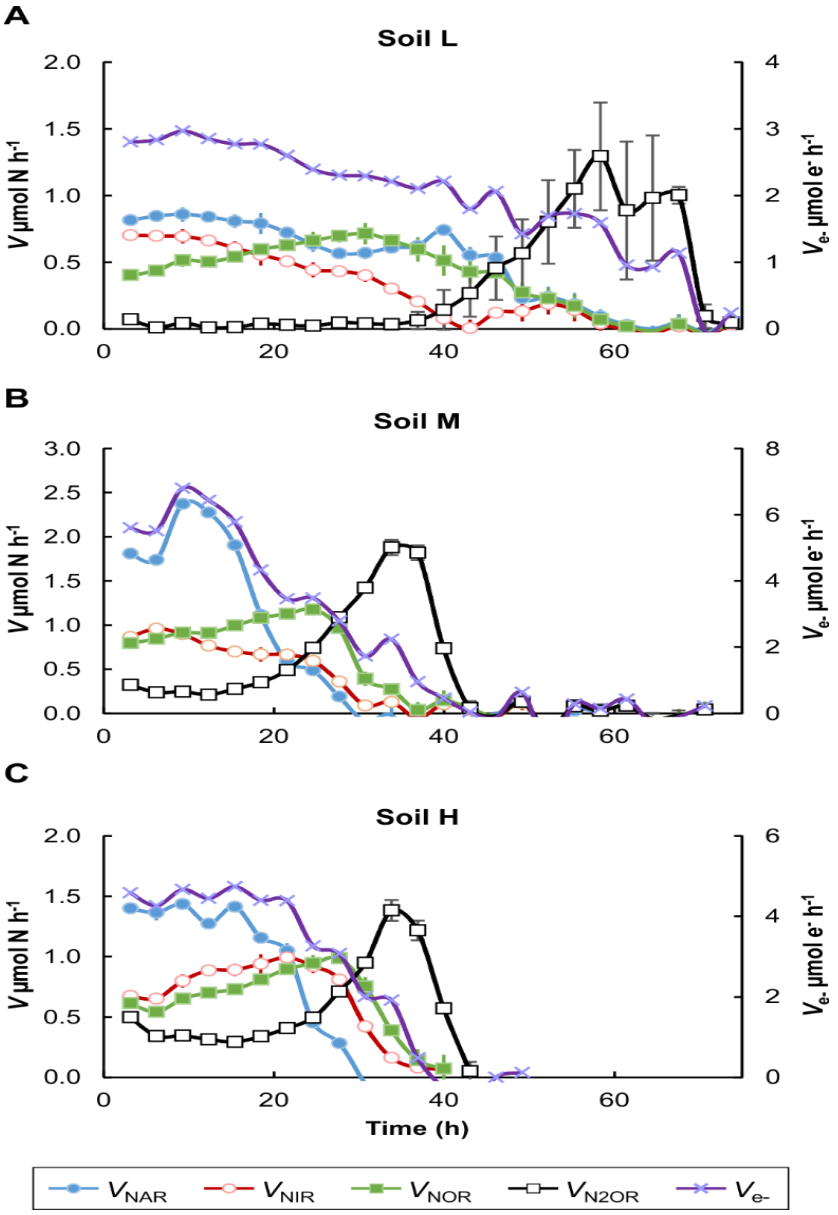

Fig. 4. Rates of individual reduction steps in denitrification. The panels show the rates of nitrate reduction (V_{NAR}), nitrite reduction (V_{NIR}), NO reduction (V_{NOR}) and N_2O reduction (V_{N2OR}), all as µmol N vial^{-1} h^{-1}. In addition, the total electron flow to denitrification is shown (V_{e-}, right axis), as µmol electrons vial^{-1} h^{-1}. The rates were based on measured net rates of production/consumption for each gas, and the rates of abiotic nitrite decay, solved for individual enzyme reactions through equations 2-7.